Full Paper

Synthesis and Discovery of Novel Pyrazole Carboxamide Derivatives as Potential Osteogenesis Inducers

Hong-Shui Lv[1]*, Qian-Qian Han[2,3]*, Xiao-Ling Ding[4], Ji-Liang Zhou[1], Pi-Shan Yang[2,3], Jun-Ying Miao[5], and Bao-Xiang Zhao[1]

[1] Institute of Organic Chemistry, School of Chemistry and Chemical Engineering, Shandong University, Jinan, P. R. China
[2] Department of Periodontology, School of Stomatology, Shandong University, Jinan, P. R. China
[3] Key Lab of Oral Biomedicine of Shandong Province, School of Stomatology, Shandong University, Jinan, P. R. China
[4] College of Advanced Professional Technology, Qingdao University, Qingdao, P. R. China
[5] School of Life Science, Shandong University, Jinan, P. R. China

A series of novel *N*-aryl-3-aryl-1-arylmethyl-1*H*-pyrazole-5-carboxamide derivatives **4a–l** was synthesized by the reaction of 3-aryl-1-arylmethyl-1*H*-pyrazole-5-carbonyl chloride with substituted aniline in good to excellent yields. Structures of the compounds were determined by IR, ^{1}H NMR, and HR-MS spectroscopy. The molecular structure was confirmed by the X-ray crystal analysis of one compound (**4j**) that was prone to crystallization. These compounds were used to induce mouse osteoblast precursors MC3T3-E1 into osteoblasts and the induction was assessed by alkaline phosphatase (ALP) activity and the gene expression of bone sialoprotein (BSP). The results showed that the compounds **4a–d**, **4g**, **4h**, and **4k** could increase the ALP activity in comparison with the negative control group and compound **4h** was the most effective one which could induce osteogenesis. Furthermore, mRNA expression of BSP which is a marker of osteogenesis was up-regulated by the compound **4h**.

Keywords: ALP activity / MC3T3-E1 / Osteogenesis / Pyrazole-5-carboxamide / Synthesis / X-ray

Received: April 27, 2012; Revised: June 20, 2012; Accepted: June 27, 2012

DOI 10.1002/ardp.201200180

Introduction

Bone is a dynamic tissue that constantly undergoes a remodeling process where bone resorption and bone deposition are balanced. Dysregulation of this coupled remodeling can lead to various diseases such as osteoporosis [1, 2], rheumatoid arthritis (RA) [3], periodontal disease [4], and other metabolic bone diseases [5–7]. Periodontal disease is a chronic infectious disease characterized by destruction of periodontal supporting tissue. It can cause significant destruction of alveolar bone, periodontal ligament (PDL), and gingiva [8]. The ultimate goal of periodontal therapy is the reproduction and reconstitution of the periodontium to restore the function of the lost periodontium. Tissue engineering is one choice of current treatment of periodontal disease, which consists of three parts: the source of seed cells for tissue engineering, suitable scaffold materials, and effective cytokines. As for cytokines, present research has focused on peptide growth factors such as BMP-2, NGF, VEGF, of which recombinant human bone morphogenetic protein-2 (BMP-2) activity was approved by the FDA in 2002 and is being used clinically as a bone graft substitute to achieve solid bony fusion and reduce the morbidity of iliac bone harvest in patients who require spine fusion surgery due to spinal instability [9, 10]. However, the application of growth factors *in vivo* is limited due to disadvantages such as the short half life, susceptibility to degradation, large side-effects, and high price [11, 12].

Small synthetic compounds are easier to manufacture than recombinant proteins and are more likely to scale-up for its

Correspondence: Bao-Xiang Zhao, Institute of Organic Chemistry, School of Chemistry and Chemical Engineering, Shandong University, Jinan 250100, P. R. China.
E-mail: bxzhao@sdu.edu.cn
Fax: +86 531 8856 4464

Additional correspondence: Prof. Pi-Shan Yang.
Email: yangps@sdu.edu.cn
Fax: +86 531 82950194
*These authors contributed equally to this work.

low cost. Small molecule compounds have a variety of biological functions and serve as cell signaling molecules, tools in molecular biology, or therapeutic drugs. Small molecule BMP stimulators that are able to bypass the need for high doses of BMP and induce bone formation have also been reported [13–15]. Therefore, the discovery of novel natural and synthetic small molecule regulators of the differentiation and maturation of osteoblasts is expected to extend clinical application of tissue engineering.

Many pyrazole derivatives are known to exhibit a wide range of biological properties such as CB1 cannabinoid receptor–ligand [16–19], inhibitor of CDK2, with good activity against a range of human tumor cell lines [20], EP1 receptor antagonists [21], trypsin-like serine protease factor Xa inhibitors [22, 23], HIV-1 integrase inhibitors [24], non-steroidal selective glucocorticoid receptor (GR) agonists and potent PPARa activators [25, 26].

As part of ongoing research directed toward the development of pyrazole-based compounds with structure diversity [27–34], we here report the synthesis of novel pyrazole carboxamides and screening aimed to discover osteogenesis inducers that promote bone regeneration instead of polypeptide growth factors or reduce the amount of polypeptide growth factors.

Results and discussion

Chemistry

The synthesis of *N*-aryl-3-aryl-1-arylmethyl-1*H*-pyrazole-5-carboxamide derivatives **4** was performed as outlined in Scheme 1 starting from ethyl 3-aryl-1-arylmethyl-1*H*-pyrazole-5-carboxylate **1** that can be synthesized as described in our previous paper [35]. Briefly, 3-aryl-1-arylmethyl-1*H*-pyrazole-5-carboxylic acid **2** was firstly obtained by alkali hydrolysis of ethyl 3-aryl-1-arylmethyl-1*H*-pyrazole-5-carboxylate **1**. 3-Aryl-1-arylmethyl-1*H*-pyrazole-5-carbonyl chloride **3** was synthesized by the reaction of carboxylic acid **2** with oxalyl chloride in CH_2Cl_2 under reflux. Then *N*-aryl-3-aryl-1-arylmethyl-1*H*-pyrazole-5-carboxamides **4** were obtained in 66.0–97.4% yield by the reaction of 3-aryl-1-arylmethyl-1*H*-pyrazole-5-carbonyl chloride **3** with substituted aniline in the presence of triethylamine in CH_2Cl_2 at room temperature. Structures of the compounds **4a–l** were determined by IR, ^{1}H NMR, and HR-MS spectroscopy.

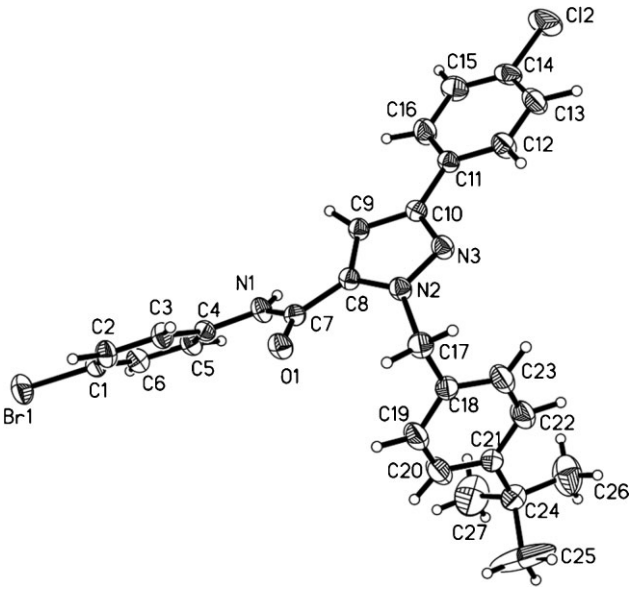

Figure 1. The molecule structure of **4j**.

Crystal structure of **4c** has been reported in our previous work [36]. Here we report the crystal structure of compound **4j** as shown in Fig. 1. A summary of crystallographic data collection parameters and refinement parameters are compiled in Table 1, meanwhile important bond lengths and

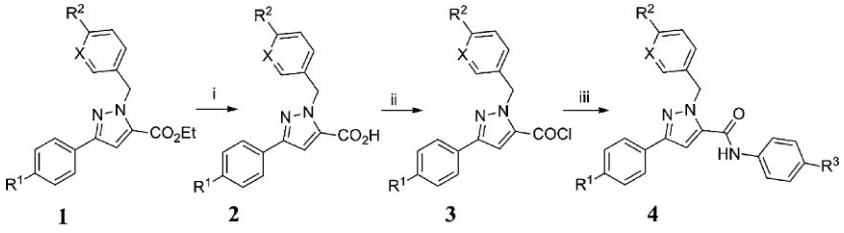

4a: R^1 = H, R^2 = Cl, X = N, R^3 = Cl
4b: R^1 = H, R^2 = Cl, X = N, R^3 = Br
4c: R^1 = H, R^2 = Cl, X = N, R^3 = EtO
4d: R^1 = H, R^2 = Cl, X = N, R^3 = MeO
4e: R^1 = H, R^2 = *tert*-Bu, X = C, R^3 = Cl
4f: R^1 = H, R^2 = *tert*-Bu, X = C, R^3 = Br
4g: R^1 = H, R^2 = *tert*-Bu, X = C, R^3 = EtO
4h: R^1 = H, R^2 = *tert*-Bu, X = C, R^3 = MeO
4i: R^1 = Cl, R^2 = *tert*-Bu, X = C, R^3 = Cl
4j: R^1 = Cl, R^2 = *tert*-Bu, X = C, R^3 = Br
4k: R^1 = Cl, R^2 = *tert*-Bu, X = C, R^3 = EtO
4l: R^1 = Cl, R^2 = *tert*-Bu, X = C, R^3 = MeO

Reagents and conditions: (i) KOH/EtOH, reflux, 4 h, then HCl aq; (ii) $(COCl)_2$ CH_2 Cl_2, reflux, 3 h; (iii) CH_2Cl_2, Et_3N, $ArNH_2$, rt, 2—3 h, 66.0—97.4% overall yields.

Scheme 1. Synthesis of *N*-aryl-3-aryl-1-arylmethyl-1*H*-pyrazole-5-carboxamide derivatives **4a–l**. Reagents and conditions: (i) KOH/EtOH, reflux, 4 h, then HCl aq; (ii) $(COCl)_2$, CH_2Cl_2, reflux, 3 h; (iii) CH_2Cl_2, Et_3N, $ArNH_2$, rt, 2–3 h, 66.0–97.4% overall yields.

Table 1. Summary of crystal data and structure refinement

	4j
Empirical formula	$C_{27}H_{25}BrClN_3O$
Formula weight	522.86
Temperature	273(2) K
Wavelength	0.71073 Å
Crystal system	Monoclinic
Space group	$P2_1/c$
Unit cell dimensions	$a = 13.673(2)$ Å, $\alpha = 90^\circ$ $b = 20.520(3)$ Å, $\beta = 104.739(3)^\circ$ $c = 9.4083(15)$ Å, $\gamma = 90^\circ$
Volume	2552.7(7) A^3
Z	4
Calculated density	1.360 Mg/m^3
Absorption coefficient	1.739 mm^{-1}
Max. and min. transmission	0.8453 and 0.7224
$F(000)$	1072
Crystal size	0.20 × 0.10 × 0.10 mm^3
θ range for data collection	1.54–26.40°
Limiting indices	$-17 \le h \le 16$, $-24 \le k \le 25$, $-11 \le l \le 10$
Reflections collected/unique	13962/5201 [R(int) = 0.0309]
Completeness to theta = 25.05	99.4%
Absorption correction	Multi-scan
Refinement method	Full-matrix least-squares on F^2
Data/restraints/parameters	5201/0/358
Goodness-of-fit on F^2	1.024
Final R indices [$I > 2\sigma(I)$]	$R_1 = 0.0424$, $wR_2 = 0.1134$
R indices (all data)	$R_1 = 0.0785$, $wR_2 = 0.1416$
Largest diff. peak and hole	0.293 and −0.356 e/$Å^3$
CCDC no.	878298

angles are depicted in Table 2. The pyrazole ring makes dihedral angles of 59.52(11), 7.51(23), and 82.56(12)° with the 4-bromophenyl, 4-chlorophenyl, and 4-*tert*-butylphenyl rings, respectively. The orientation of the 4-bromophenyl moiety is defined by the torsion angle of C(4)-N(1)-C(7)-C(8) −169.7(3)°. The packing diagram of **4j** is shown in Fig. 2. The molecules of **4j** are stabilized by intramolecular C–H···O and C–H···N bonds, meanwhile linked by intermolecular C–H···O, C–H···Cl, and N–H···O bonds (shown in Table 3).

Table 2. Selected bond lengths (Å), bond angles (°), and torsion angles (°) of compound **4j**

C(10)–C(11)	**1.467(4)**	**C(7)–C(8)**	**1.476(4)**
C(9)–C(10)	1.403(4)	C(9)–C(8)	1.368(4)
N(2)–C(8)	1.361(4)	N(2)–N(3)	1.348(3)
N(3)–C(10)	1.341(3)	N(2)–C(17)	1.480(4)
C(18)–C(17)	1.504(5)	N(1)–C(7)	1.356(4)
N(1)–C(4)	1.411(3)	O(1)–C(7)	1.238(3)
C(10)–N(3)–N(2)	105.4(2)	N(3)–N(2)–C(8)	111.7(2)
N(1)–C(7)–C(8)	113.1(2)	C(7)–N(1)–C(4)	127.3(2)
N(2)–C(17)–C(18)	110.9(2)	O(1)–C(7)–C(8)	123.2(2)
C(4)–N(1)–C(7)–C(8)	−169.7(3)	C(8)–N(2)–C(17)–C(18)	80.7(4)
C(19)–C(18)–C(17)–N(2)	−104.8(4)	C(23)–C(18)–C(17)–N(2)	75.2(4)

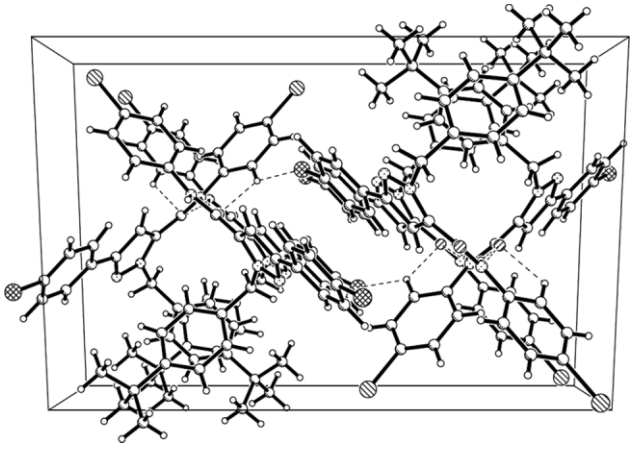

Figure 2. A packing diagram of the crystal structure of **4j**.

Table 3. Hydrogen bond geometry (Å, °)

D–H···A	**D–H**	**H···A**	**D···A**	**D–H···A**
N1–H1···O1^{i}	0.81	2.16	2.937(3)	160
Intra C3–H3···O1	0.97	2.49	2.961(4)	110
C5–H5···Cl2^{ii}	1.05	2.71	3.478(3)	130
C5–H5···O1^{i}	1.05	2.50	3.304(3)	133
Intra C12–H12···N3	0.80	2.60	2.868(4)	102
Intra C17–H17A···O1	0.92	2.45	3.082(4)	126

Symmetry code: (i) x, $(1/2) - y$, $(1/2) + z$; (ii) $-1 + x$, $(1/2) - y$, $(3/2) - z$.
D and A are the hydrogen-bond donor and acceptor, respectively.

Effects of compounds 4a–l on cellular alkaline phosphatase (ALP) activity

Mouse osteoblast precursor MC3T3-E1 is a widely accepted cell line that can be used to study the role of bone formation *in vitro*. ALP is widely considered to be the marker of the differentiation and function of the osteoblast [37]. ALP activity is an early osteogenic marker and the testing methods are relatively simple. When ST2 cells were treated with BMP-2 at concentrations over 10 ng/mL for 6 days, ALP activity was significantly increased [38]. ST2 is a mouse bone marrow stromal stem cell line and MC3T3-E1 is a mouse osteoblast precursor. Both cells have the potential to differentiate into osteoblasts. In our present research, we chose MC3T3-E1 cells as cell model and detected the ALP activity after exposing to compounds **4a–l** for 7 days. As shown in Fig. 3, compounds **4a–d**, **4g**, **4h**, and **4k** could increase the ALP activity in comparison with the negative control group. Among them, compound **4h** exhibited higher ALP activity than other groups. The results showed that compound **4h** might have a relatively strong osteoinduction effect.

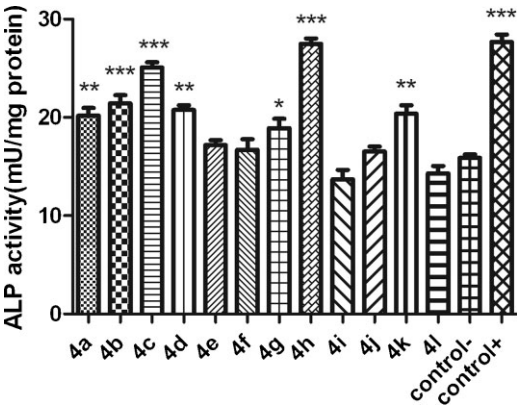

Figure 3. Effect of pyrazole carboxamide derivatives **4a–l** on ALP activity of MC3T3-E1, an early marker of osteogenic differentiation, after culturing cells for 7 days in growth medium. Control−, medium with 4 μM DMSO; **4a–l**, medium supplemented with compound **4a–l**; Control+, osteogenetic medium. $^{*}p < 0.05$, $^{**}p < 0.01$, $^{***}p < 0.001$.

Effects of compound 4h on cellular alkaline phosphatase (ALP) activity and cell viability

Next, the effect of the compound **4h** at different concentrations on ALP activity was assessed. As shown in Fig. 4, when cells were treated with various concentrations of compound **4h** for 7 days, cellular alkaline phosphatase (ALP) activity was affected and the result showed that compound **4h** at the concentration of 4 μmol/L exhibited the highest ALP activity.

Cell proliferation and differentiation are two relatively independent processes. Several studies confirmed that a variety of cytokines or compounds could inhibit cell proliferation but promote cell differentiation [39, 40]. Therefore, we use MTT to detect the effect of compound **4h** on cell proliferation *in vitro*. MTT results (Fig. 5) showed that cell viability depended on the concentration of compound **4h** significantly. When treated with 1 and 4 μM of compound **4h** for 24 h, the cell viability of MC3T3-E1 was 90.9 ± 1.50 and 87.9 ± 5.63%, respectively, which was not changed obviously. Moreover, when cells were treated with 1 and 4 μM of compound **4h** for 48 h, the cell viability of MC3T3-E1 was 89.5 ± 2.69 and 86.9 ± 2.58%, respectively, which was also not changed notably. However, when cells were treated with 16 and 40 μM of compound **4h** for 24 h, the cell viability of MC3T3-E1 (80.3 ± 6.10, 67.1 ± 6.20%, respectively) was decreased significantly. When cells were treated for 48 h, the cell viability decreased more significantly (57.9 ± 3.80, 55.7 ± 1.81%, respectively). Therefore, we believed that the selected 4 μM of compound **4h** was suitable for a further study.

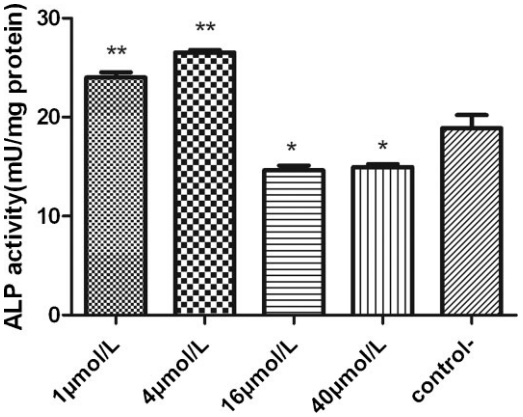

Figure 4. Effect of compound **4h** at different concentrations on ALP activity of MC3T3-E1 after culturing confluent cells for 7 days in medium containing different concentrations of compound **4h**. Control−, medium with 4 μmol/L DMSO; $^{*}p < 0.01$, $^{**}p < 0.001$.

Effect of compound 4h on mRNA expression level of BSP

Bone sialoprotein (BSP) is a highly post-translationally modified protein which is an abundant non-collagenous component of the bone matrix and it is a marker of osteogenesis. BSP expression was up-regulated when human dental pulp stem cells (DPSCs) were induced into osteoblasts [41], and ALP activity and BSP level were down-regulated when compounds were used to suppress osteoblastic differentiation and mineralized nodule formation [42]. To further determine the effect of compound **4h** on osteoinduction activity of MC3T3-E1 cells, total RNA was isolated, and RT-PCR was performed to measure gene expression levels of BSP. As shown in Fig. 6, we found that in the compound **4h** induced group, the mRNA expression levels of BSP showed a 1.69-fold increase compared with that in the negative control group after 4 days induction. The increase was similar to that of the positive control group which was a 1.73-fold increase compared with the negative control group.

Conclusion

A series of novel *N*-aryl-3-aryl-1-arylmethyl-1*H*-pyrazole-5-carboxamide derivatives **4a–4l** was synthesized and characterized by IR, ^{1}H NMR, and HRMS spectroscopy. The molecular structure was confirmed by X-ray crystal analysis of one compound (**4j**). These compounds were used to induce differentiation of mouse osteoblast precursors MC3T3-E1 into osteoblasts and the induction was assessed by ALP activity and mRNA expression of BSP. The results showed that the compounds **4a–d**, **4g**, **4h**, and **4k** could increase the ALP activity in comparison with the negative control group and compound **4h** was the most effective one. Furthermore, the mRNA

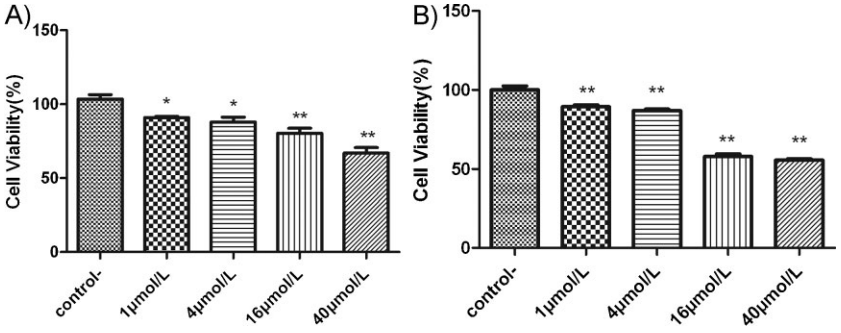

Figure 5. Effects of compound **4h** at different concentrations (1, 4, 16, and 40 μM) on viability of MC3T3-E1 cells treated for 24 h (A) and 48 h (B). Control−, medium. $^{*}p < 0.05$, $^{**}p < 0.01$.

expression of BSP which is a marker of osteogenesis was up-regulated by compound **4h**. Therefore, compound **4h** may have the osteoinduction activity for MC3T3-E1 cells. Currently, investigations are underway to elucidate the osteoinduction activity and the mechanism by which compound **4h** promotes osteogenetic differentiation on MC3T3-E1 and the results will be reported in due course.

Experimental

All reagents were of analytical grade or chemically pure. Analytical TLC was performed on silica gel 60 F_{254} plates (*Merck KGaA*). m.p. was determined on an *XD-4* digital micromelting point apparatus. ^{1}H NMR spectra were recorded on a Bruker Avance 400 spectrometer, using $CDCl_3$ as solvent and TMS as internal standard. IR spectra were recorded with an IR spectrophotometer Avtar 370 FT-IR (Termo Nicolet). HRMS spectra were recorded on a LTQ Orbitrap Hybrid mass spectrometer.

3-Aryl-1-arylmethyl-1H-pyrazole-5-carbonyl chloride ***3***

The starting material ethyl 3-aryl-1-arylmethyl-1*H*-pyrazole-5-carboxylate (**1**) was synthesized as described in our previous paper [35]. To a solution of **1** (10 mmol) in ethanol (50 mL) was added KOH (30 mmol). The mixture was refluxed for 2 h. After cooling, ethanol was removed under reduced pressure. The residue was dissolved in 50 mL water. The solution was added hydrochloric acid (3 M) until pH = 4–5. The precipitate was filtered and dried to give 3-aryl-1-arylmethyl-1*H*-pyrazole-5-carboxylic acid (**2**) as pure product in 100% yield. A solution of **2** (1 mmol), oxalyl chloride (0.5 mL), and two drops of DMF in CH_2Cl_2 (10 mL) was refluxed for 4 h. After cooling, the solvent was removed to give **3**, which was used without further purification.

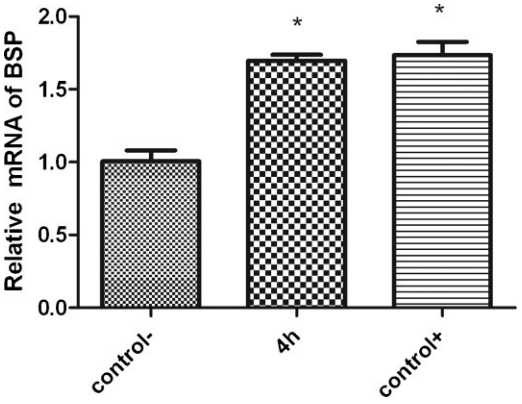

Figure 6. Effects of compound **4h** on BSP expression in MC3T3-E1 osteoblastic cells analyzed by RT-PCR. 4h, medium with 4 μM compound **4h**; Control−, medium with 4 μM DMSO; Control+, osteogenetic medium. $^{*}p < 0.01$.

N-Aryl-3-aryl-1-arylmethyl-1H-pyrazole-5-carboxamide ***4***

To a solution of substituted aniline (1 mmol) in CH_2Cl_2 (10 mL) containing Et_3N (0.5 mL), 3-aryl-1-arylmethyl-1*H*-pyrazole-5-carbonyl chloride (**3**) (1 mmol) dissolved in CH_2Cl_2 (5 mL) was added dropwise at room temperature. The mixture was stirred overnight. The end of reaction was detected by TLC. After which the solution was washed by water (15 mL × 2), the water phase was extracted with CH_2Cl_2 (15 mL × 1). The combined organic phase was dried over $MgSO_4$. After filtration, the solvent was removed under reduced pressure. The residue was purified by column chromatography on silica gel using PE/EtOAc as an eluent to afford title compound **4** in 66.0–97.4% (overall yields).

N-(4-Chlorophenyl)-1-((6-chloropyridin-3-yl)methyl)-3-phenyl-1H-pyrazole-5-carboxamide ***4a***

White solid, yield: 66.0%, m.p.: 214–216°C, IR: ν_{max} cm^{-1} 3412 (N–H), 1674 (C=O). ^{1}H NMR ($CDCl_3$, 400 MHz): 5.82 (s, 2H, $-CH_2$), 7.06 (s, 1H, pyrazole–H), 7.26 (d, 1H, J = 8.1 Hz, pyridine–H), 7.34 (d, 2H, J = 8.7 Hz, Ar–H), 7.36–7.47 (m, 3H, Ar–H), 7.56 (d, 2H, J = 8.7 Hz, Ar–H), 7.74 (dd, 1H, J_1 = 8.1 Hz, J_2 = 2.2 Hz, pyridine–H), 7.81 (d, 2H, J = 7.4 Hz, Ar–H), 7.93 (s, 1H, N–H), 8.47 (d, 1H, J = 2.2 Hz, pyridine–H); HRMS calcd for $[M+H]^+$ $C_{22}H_{17}Cl_2N_4O$: 423.0779, found 423.0769.

N-(4-Bromophenyl)-1-((6-chloropyridin-3-yl)methyl)-3-phenyl-1H-pyrazole-5-carboxamide ***4b***

White solid, yield: 72.8%, m.p.: 194–198°C, IR: ν_{max} cm^{-1} 3412 (N–H), 1675 (C=O). ^{1}H NMR ($CDCl_3$, 400 MHz): 5.81 (s, 2H, $-CH_2$), 6.96 (s, 1H, pyrazole–H), 7.26 (d, 1H, J = 8.2 Hz, pyridine–H), 7.33–7.54 (m, 7H, Ar–H), 7.69 (s, 1H, N–H), 7.73 (dd, 1H, J_1 = 8.2 Hz, J_2 = 2.3 Hz, pyridine–H), 7.80 (d, 2H, J = 7.1 Hz, Ar–H), 8.48 (d, 1H, J = 2.2 Hz, pyridine–H); HRMS calcd for $[M+H]^+$ $C_{22}H_{17}BrClN_4O$: 467.0274, found 467.0261.

1-((6-Chloropyridin-3-yl)methyl)-N-(4-ethoxyphenyl)-3-phenyl-1H-pyrazole-5-carboxamide ***4c***

Yellow solid, yield: 77.7%, m.p.: 164–165°C, IR: ν_{max} cm^{-1} 3339 (N–H), 1663 (C=O). ^1H NMR ($CDCl_3$, 400 MHz): 1.42 (t, 3H, J = 7.0 Hz, $-CH_3$), 4.03 (q, 2H, J = 7.0 Hz, $-OCH_2$), 5.82 (s, 2H, $-CH_2$), 6.90 (d, 2H, J = 8.9 Hz, Ar–H), 6.93 (s, 1H, pyrazole–H), 7.24 (d, 1H, J = 8.2 Hz, pyridine–H), 7.32–7.39 (m, 1H, Ar–H), 7.39–7.48 (m, 4H, Ar–H), 7.63 (s, 1H, N–H), 7.74 (dd, 1H, J_1 = 8.2 Hz, J_2 = 2.3 Hz, pyridine–H), 7.79 (d, 2H, J = 7.2 Hz, Ar–H), 8.48 (d, 1H, J = 2.3 Hz, pyridine–H); HRMS calcd for $[M+H]^+$ $C_{24}H_{22}ClN_4O_2$: 433.1431, found 433.1425.

1-((6-Chloropyridin-3-yl)methyl)-N-(4-methoxyphenyl)-3-phenyl-1H-pyrazole-5-carboxamide ***4d***

Yellow solid, yield: 75.9%, m.p.: 118–121°C, IR: ν_{max} cm^{-1} 3359 (N–H), 1666 (C=O). ^1H NMR ($CDCl_3$, 400 MHz): 3.82 (s, 3H, $-OCH_3$), 5.82 (s, 2H, $-CH_2$), 6.91 (d, 2H, J = 8.9 Hz, Ar–H), 6.94 (s, 1H, pyrazole–H), 7.24 (d, 1H, J = 8.2 Hz, pyridine–H), 7.33–7.39 (m, 1H, Ar–H), 7.39–7.50 (m, 4H, Ar–H), 7.64 (s, 1H, N–H), 7.74 (dd, 1H, J_1 = 8.2 Hz, J_2 = 2.3 Hz, pyridine–H), 7.80 (d, 2H, J = 7.2 Hz, Ar–H), 8.48 (d, 1H, J = 2.3 Hz, pyridine–H); HRMS calcd for $[M+H]^+$ $C_{23}H_{20}ClN_4O_2$: 419.1275, found 419.1276.

1-(4-(Tert-butyl)benzyl)-N-(4-chlorophenyl)-3-phenyl-1H-pyrazole-5-carboxamide ***4e***

Yellow solid, yield: 73.6%, m.p.: 182–183°C, IR: ν_{max} cm^{-1} 3372 (N–H), 1654 (C=O). ^1H NMR ($CDCl_3$, 400 MHz): 1.26 (s, 9H, $-C(CH_3)_3$), 5.78 (s, 2H, $-CH_2$), 6.90 (s, 1H, pyrazole–H), 7.26–7.37 (m, 7H, Ar–H), 7.37–7.45 (m, 2H, Ar–H), 7.49 (d, 2H, J = 8.7 Hz, Ar–H), 7.65 (s, 1H, N–H), 7.81 (d, 2H, J = 7.2 Hz, Ar–H); HRMS calcd for $[M+H]^+$ $C_{27}H_{27}ClN_3O$: 444.1843, found 444.1848.

N-(4-Bromophenyl)-1-(4-(tert-butyl)benzyl)-3-phenyl-1H-pyrazole-5-carboxamide ***4f***

Yellow solid, yield: 81.0%, m.p.: 175–178°C, IR: ν_{max} cm^{-1} 3276 (N–H), 1656 (C=O). ^1H NMR ($CDCl_3$, 400 MHz): 1.26 (s, 9H, $-C(CH_3)_3$), 5.78 (s, 2H, $-CH_2$), 6.91 (s, 1H, pyrazole–H), 7.27–7.32 (m, 4H, Ar–H), 7.32–7.37 (m, 1H, Ar–H), 7.38–7.48 (m, 6H, Ar–H), 7.65 (s, 1H, N–H), 7.81 (d, 2H, J = 7.8 Hz, Ar–H); HRMS calcd for $[M+H]^+$ $C_{27}H_{27}BrN_3O$: 488.1338, found 488.1329.

1-(4-(Tert-butyl)benzyl)-N-(4-ethoxyphenyl)-3-phenyl-1H-pyrazole-5-carboxamide ***4g***

Yellow solid, yield: 74.2%, m.p.: 149–151°C, IR: ν_{max} cm^{-1} 3267 (N–H), 1645 (C=O). ^1H NMR ($CDCl_3$, 400 MHz): 1.26 (s, 9H, $-C(CH_3)_3$), 1.40 (t, 3H, J = 7.0 Hz, $-CH_3$), 4.01 (q, 2H, J = 7.0 Hz, $-OCH_2$), 5.78 (s, 2H, $-CH_2$), 6.83–6.93 (m, 3H, pyrazole–H + Ar–H), 7.27–7.36 (m, 5H, Ar–H), 7.36–7.47 (m, 4H, Ar–H), 7.65 (s, 1H, N–H), 7.81 (d, 2H, J = 7.2 Hz, Ar–H); HRMS calcd for $[M+H]^+$ $C_{29}H_{32}N_3O_2$: 454.2495, found 454.2497.

1-(4-(Tert-butyl)benzyl)-N-(4-methoxyphenyl)-3-phenyl-1H-pyrazole-5-carboxamide ***4h***

White solid, yield: 75.6%, m.p.: 164–167°C, IR: ν_{max} cm^{-1} 3261 (N–H), 1646 (C=O). ^1H NMR ($CDCl_3$, 400 MHz): 1.26 (s, 9H, $-C(CH_3)_3$), 3.81 (s, 3H, $-OCH_3$), 5.80 (s, 2H, $-CH_2$), 6.87–6.93 (m, 3H, pyrazole–H + Ar–H), 7.28–7.32 (m, 4H, Ar–H), 7.32–7.36 (m, 1H, Ar–H), 7.38–7.47 (m, 4H, Ar–H), 7.57 (s, 1H, N–H), 7.82 (d, 2H, J = 7.6 Hz, Ar–H); HRMS calcd for $[M+H]^+$ $C_{28}H_{30}N_3O_2$: 440.2338, found 440.2338.

1-(4-(Tert-butyl)benzyl)-N,3-bis(4-chlorophenyl)-1H-pyrazole-5-carboxamide ***4i***

White solid, yield: 68.6%, m.p.: 213–215°C, IR: ν_{max} cm^{-1} 3283 (N–H), 1658 (C=O). ^1H NMR ($CDCl_3$, 400 MHz): 1.26 (s, 9H, $-C(CH_3)_3$), 5.78 (s, 2H, $-CH_2$), 6.88 (s, 1H, pyrazole–H), 7.28–7.42 (m, 6H, Ar–H), 7.38 (d, 2H, J = 8.1 Hz, Ar–H), 7.50 (d, 2H, J = 8.6 Hz, Ar–H), 7.62 (s, 1H, N–H), 7.75 (d, 2H, J = 8.1 Hz, Ar–H); HRMS calcd for $[M+H]^+$ $C_{27}H_{26}Cl_2N_3O$: 478.1453, found 478.1450.

N-(4-Bromophenyl)-1-(4-(tert-butyl)benzyl)-3-(4-chlorophenyl)-1H-pyrazole-5-carboxamide ***4j***

Yellow solid, yield: 97.4%, m.p.: 202–206°C, IR: ν_{max} cm^{-1} 3283 (N–H), 1659 (C=O). ^1H NMR ($CDCl_3$, 400 MHz): 1.26 (s, 9H, $-C(CH_3)_3$), 5.77 (s, 2H, $-CH_2$), 6.88 (s, 1H, pyrazole–H), 7.27–7.34 (m, 4H, Ar–H), 7.38 (d, 2H, J = 8.5 Hz, Ar–H), 7.42–7.50 (m, 4H, Ar–H), 7.63 (s, 1H, N–H), 7.74 (d, 2H, J = 8.5 Hz, Ar–H); HRMS calcd for $[M+H]^+$ $C_{27}H_{26}BrClN_3O$: 522.0948, found 522.0935.

1-(4-(Tert-butyl)benzyl)-3-(4-chlorophenyl)-N-(4-ethoxyphenyl)-1H-pyrazole-5-carboxamide ***4k***

Yellow solid, yield: 84.6%, m.p.: 185–187°C, IR: ν_{max} cm^{-1} 3275 (N–H), 1649 (C=O). ^1H NMR ($CDCl_3$, 400 MHz): 1.27 (s, 9H, $-C(CH_3)_3$), 1.41 (t, 3H, J = 7.0 Hz, $-CH_3$), 4.03 (q, 2H, J = 7.0 Hz, $-OCH_2$), 5.79 (s, 2H, $-CH_2$), 6.87 (s, 1H, pyrazole–H), 6.89 (d, 2H, J = 9.0 Hz, Ar–H), 7.28–7.34 (m, 4H, Ar–H), 7.38 (d, 2H, J = 8.5 Hz, Ar–H), 7.42 (d, 2H, J = 8.5 Hz, Ar–H), 7.53 (s, 1H, N–H), 7.75 (d, 2H, J = 8.5 Hz, Ar–H); HRMS calcd for $[M+H]^+$ $C_{29}H_{31}ClN_3O_2$: 488.2105, found 488.2107.

1-(4-(Tert-butyl)benzyl)-3-(4-chlorophenyl)-N-(4-methoxyphenyl)-1H-pyrazole-5-carboxamide ***4l***

Yellow solid, yield: 89.6%, m.p.: 201–203°C, IR: ν_{max} cm^{-1} 3283 (N–H), 1653 (C=O). ^1H NMR ($CDCl_3$, 400 MHz): 1.27 (s, 9H, $-C(CH_3)_3$), 3.81 (s, 3H, $-OCH_3$), 5.78 (s, 2H, $-CH_2$), 6.87 (s, 1H, pyrazole–H), 6.89 (d, 2H, J = 8.5 Hz, Ar–H), 7.28–7.34 (m, 4H, Ar–H), 7.38 (d, 2H, J = 8.5 Hz, Ar–H), 7.44 (d, 2H, J = 8.6 Hz, Ar–H), 7.55 (s, 1H, N–H), 7.75 (d, 2H, J = 8.5 Hz, Ar–H); HRMS calcd for $[M+H]^+$ $C_{28}H_{29}ClN_3O_2$: 474.1948, found 474.1952.

Crystal structure determination of compound 4j

Suitable single crystals of **4j** for X-ray structural analysis were obtained by recrystallization from dichloromethane/ethyl acetate. The diffraction data was collected with a Bruker SMART CCD diffractometer using a graphite monochromated Mo Kα radiation (λ = 0.71073 Å) at 273(2) K. The structures were solved by direct methods with the SHELXS-97 program and refinements on F^2 were performed with the SHELXL-97 [43] program by full-matrix least-squares techniques with anisotropic thermal parameters for the non-hydrogen atoms. All H atoms were initially located in a difference Fourier map. The methyl H atoms were then constrained to an ideal geometry, with C–H = 0.96 Å and U*iso*(H) = 1.5 Ueq(C). All other H atoms were placed in geometrically idealized positions and constrained to ride on their parent atoms, with C–H = 0.93 Å and U*iso*(H) = 1.2 Ueq(C).

Cell culture and ALP activity of compounds 4a–l

MC3T3-E1 cells were cultured in α-MEM (Hyclone, USA) supplemented with 10% FBS (Gibco, USA), 100 units/mL penicillin, and 100 μg/mL streptomycin. When reaching 80% confluence, the cells were seeded at a density of 2×10^4 cells/well on 24-well plates and allowed to grow to confluence. Then cells were maintained in compounds-stimulated media [α-MEM with 10% v/v FBS, supplemented with different kinds of compounds **4a–l** (4 μmol/L)]. Cells cultured on basic media supplemented with 4 μmol/L of DMSO were the negative control and cells cultured in osteogenic media (α-MEM supplemented with 10^{-8} mol/L dexamethasone, 50 mg/L ascorbic acid, and 10 mmol/L β-glycerophosphate) were the positive control. Media were changed every 2 days. After 7 days of induction, cells were washed with 0.01 mol/L PBS and scraped into 100 μL of 0.2% TritonX-100. Then cells were sonicated and cell lysates were centrifuged at 14 000 *g* for 10 min at 4°C. ALP activity in the supernatant was assayed according to the instructions of the manufacturer (Nanjing Jiancheng, China). Results were adjusted according to protein content detected by BCA standard (KeyGEN BioTECH, China).

ALP activity of compound 4h at different concentrations

MC3T3-E1 were cultured in α-MEM supplemented with 10% FBS. When reaching 80% confluence, cells were seeded in 6-well plates at a density of 1×10^5 cells/well. Then the media were replaced with fresh α-MEM containing different concentrations of compound **4h** (0, 1, 4, 16, and 40 μmol/L) for 7 days. Media were changed every 2 days. After 7 days of induction, ALP activity was detected.

MTT assay

MC3T3-E1 were cultured in α-MEM supplemented with 10% FBS. When reaching 80% confluence, cells were seeded in 96-well plates at a density of 1×10^4 cells/well. Then the media were replaced with fresh α-MEM containing different concentrations of compound **4h** (0, 1, 4, 16, and 40 μmol/L) for 24 or 48 h. Then, 200 μL culture medium containing 20 μL MTT (5 mg/mL) was added to each well and the cells were incubated for 4 h at 37°C. The supernatant was removed and 150 μL of DMSO was added to each well. Absorbance at 490 nm was measured in a multiwell spectrophotometer (BioRad, USA). The results were determined by five independent experiments.

Real-time RT-PCR analysis

MC3T3-E1 were cultured in α-MEM supplemented with 10% FBS. When reaching 80% confluence, cells were seeded in 6-well plates at a density of 1×10^5 cells/well. Then the media were replaced with fresh α-MEM containing 4 μmol/L compound **4h**. After 4 days of induction, total RNA was isolated using Trizol reagent (TaKaRa Biotech, Japan) from MC3T3-E1 cells with different treatments and used for cDNA synthesis using Reverse Transcriptase (TaKaRa Biotech, Japan). Real-time reverse transcription-PCR (qRT-PCR) analysis was performed using 1 μL of cDNA in a 20 μL reaction volume with Roche 480 in triplicate. The relative expression level of the housekeeping gene GAPDH was used to normalize gene expression in each sample in different groups. The sequences of the primers for amplication of mouse BSP and GAPDH are listed in Table 4.

Table 4. The sequences of the primers for amplication of mouse BSP and GAPDH

Primer	Sequence
GAPDH	Forward: 5′-AGGTCGGTGTGAACGGATTTG-3′ Reverse: 5′-TGTAGACCATGTAGTTGAGGTCA-3′
BSP	Forward: 5′-CAGGGAGGCAGTGACTCTTC-3′ Reverse: 5′-AGTGTGGAAAGTGTGGCGTT-3′

Statistical analysis

Results were presented as the means ± SD of three to five replicates for each experiment. The statistical significance of the differences between different groups was assessed by one-way ANOVA. $p < 0.05$ was considered as statistically significant.

This work was supported by National Natural Science Foundation of China (20972088, 90813022, and 81070835) and the Independent Innovation Foundation of Shandong University (2009JC007).

The authors have declared no conflict of interest.

References

[1] F. Fulfaro, A. Casuccio, C. Ticozzi, C. Ripamonti, *Pain* **1998**, *78*, 157–169.

[2] V. Gangji, T. Appelboom, *Clin. Rheumatol.* **1999**, *18*, 266–267.

[3] T. Braun, J. Zwerina, *Arthritis Res. Ther.* **2011**, *13*, 235.

[4] A. Yoshihara, T. Deguchi, H. Miyazaki, *Community Dent. Health* **2011**, *28*, 165–169.

[5] R. Bargman, R. Posham, A. L. Boskey, E. Dicarlo, C. Raggio, N. Pleshko, *Osteoporos. Int.* **2012**, *23*, 1141–1150.

[6] A. H. Undale, J. J. Westendorf, M. J. Yaszemski, S. Khosla, *Mayo Clin. Proc.* **2009**, *84*, 893–902.

[7] A. H. El-Gharbawy, J. N. Peeden, Jr., R. S. Lachman, J. M. Graham, Jr., S. R. Moore, D. L. Rimoin, *Am. J. Med. Genet. Part A* **2010**, *152A*, 169–174.

[8] D. L. Wolf, I. B. Lamster, *Dent. Clin. North Am.* **2011**, *55*, 47–61.

[9] S. D. Boden, T. A. Zdeblick, H. S. Sandhu, S. E. Heim, *Spine (PhilaPa 1976)* **2000**, *25*, 376–381.

[10] E. E. Johnson, M. R. Urist, *Clin. Orthop. Relat. Res.* **2000**, *371*, 61–74.

[11] D. H. Thamm, I. D. Kurzman, M. A. Clark, E. J. Ehrhart, III, S. L. Kraft, D. L. Gustafson, D. M. Vail, *Clin. Cancer Res.* **2010**, *16*, 1498–1508.

[12] R. M. Olabisi, Z. Lazard, M. H. Heggeness, K. M. Moran, J. A. Hipp, A. K. Dewan, A. R. Davis, J. L. West, E. A. Olmsted-Davis, *Spine J.* **2011**, *11*, 545–556.

[13] K. W. Park, H. Waki, W. K. Kim, B. S. Davies, S. G. Young, F. Parhami, P. Tontonoz, *Mol. Cell. Biol.* **2009**, *29*, 3905–3914.

[14] S. Kato, S. Sangadala, K. Tomita, L. Titus, S. D. Boden, *Mol. Cell. Biochem.* **2011**, *349*, 97–106.

[15] M. Okada, S. Sangadala, Y. Liu, M. Yoshida, B. V. Reddy, L. Titus, S. D. Boden, *Cell Biochem. Funct.* **2009**, *27*, 526–534.

[16] H. J. Seo, M. J. Kim, S. H. Lee, M. E. Jung, M. S. Kim, K. Ahn, J. Kim, J. Lee, *Bioorg. Med. Chem.* **2010**, *18*, 1149–1162.

[17] R. Silvestri, A. Ligresti, G. La Regina, F. Piscitelli, V. Gatti, A. Lavecchia, A. Brizzi, S. Pasquini, M. Allara, N. Fantini, M. A. Carai, C. Bigogno, M. G. Rozio, R. Sinisi, E. Novellino, G. Colombo, V. Di Marzo, G. Dondio, F. Corelli, *Eur. J. Med. Chem.* **2010**, *45*, 5878–5886.

[18] S. R. Donohue, R. F. Dannals, C. Halldin, V. W. Pike, *J. Med. Chem.* **2011**, *54*, 2961–2970.

[19] P. K. Sasmal, D. S. Reddy, R. Talwar, B. Venkatesham, D. Balasubrahmanyam, M. Kannan, P. Srinivas, K. S. Kumar, B. N. Devi, V. P. Jadhav, S. K. Khan, P. Mohan, H. Chaudhury, D. Bhuniya, J. Iqbal, R. Chakrabarti, *Bioorg. Med. Chem. Lett.* **2011**, *21*, 562–568.

[20] P. G. Wyatt, A. J. Woodhead, V. Berdini, J. A. Boulstridge, M. G. Carr, D. M. Cross, D. J. Davis, L. A. Devine, T. R. Early, R. E. Feltell, E. J. Lewis, R. L. McMenamin, E. F. Navarro, M. A. O'Brien, M. O'Reilly, M. Reule, G. Saxty, L. C. Seavers, D. M. Smith, M. S. Squires, G. Trewartha, M. T. Walker, A. J. Woolford, *J. Med. Chem.* **2008**, *51*, 4986–4999.

[21] A. Hall, A. Billinton, A. K. Bristow, S. H. Brown, A. Chowdhury, L. Cutler, G. M. Giblin, P. Goldsmith, T. G. Hayhow, I. R. Kilford, A. Naylor, B. Passingham, D. A. Rawlings, *Bioorg. Med. Chem. Lett.* **2008**, *18*, 4027–4032.

[22] J.-X. Qiao, S. R. King, K. He, P. C. Wong, A. R. Rendina, J. M. Luettgen, B. Xin, R. M. Knabb, R. R. Wexler, P. Y. Lam, *Bioorg. Med. Chem. Lett.* **2009**, *19*, 462–468.

[23] J.-X. Qiao, D. L. Cheney, R. S. Alexander, A. M. Smallwood, S. R. King, K. He, A. R. Rendina, J. M. Luettgen, R. M. Knabb, R. R. Wexler, P. Y. Lam, *Bioorg. Med. Chem. Lett.* **2008**, *18*, 4118–4123.

[24] H. M. Langford, P. D. Williams, C. F. Homnick, J. P. Vacca, P. J. Felock, K. A. Stillmock, M. V. Witmer, D. J. Hazuda, L. J. Gabryelski, W. A. Schleif, *Bioorg. Med. Chem. Lett.* **2008**, *18*, 721–725.

[25] H. A. Barnett, D. M. Coe, T. W. Cooper, T. I. Jack, H. T. Jones, S. J. Macdonald, I. M. McLay, N. Rayner, R. Z. Sasse, T. J. Shipley, P. A. Skone, G. I. Somers, S. Taylor, I. J. Uings, J. M. Woolven, G. G. Weingarten, *Bioorg. Med. Chem. Lett.* **2009**, *19*, 158–162.

[26] M. Alvarado, P. Goya, M. Macias-Gonzalez, F. J. Pavon, A. Serrano, N. Jagerovic, J. Elguero, A. Gutierrez-Rodriguez, S. Garcia-Granda, M. Suardiaz, F. Rodriguez de Fonseca, *Bioorg. Med. Chem.* **2008**, *16*, 10098–10105.

[27] F. Wei, B.-X. Zhao, B. Huang, L. Zhang, C.-H. Sun, W.-L. Dong, D.-S. Shin, J.-Y. Miao, *Bioorg. Med. Chem. Lett.* **2006**, *16*, 6342–6347.

[28] Y. Xia, Z.-W. Dong, B.-X. Zhao, X. Ge, N. Meng, D.-S. Shin, J.-Y. Miao, *Bioorg. Med. Chem.* **2007**, *15*, 6893–6899.

[29] C.-D. Fan, B.-X. Zhao, F. Wei, G.-H. Zhang, W.-L. Dong, J.-Y. Miao, *Bioorg. Med. Chem. Lett.* **2008**, *18*, 3860–3864.

[30] Y. Xia, C.-D. Fan, B.-X. Zhao, J. Zhao, D.-S. Shin, J.-Y. Miao, *Eur. J. Med. Chem.* **2008**, *43*, 2347–2353.

[31] S. Lian, H. Su, B.-X. Zhao, W.-Y. Liu, L.-W. Zheng, J.-Y. Miao, *Bioorg. Med. Chem.* **2009**, *17*, 7085–7092.

[32] X.-L. Ding, H.-Y. Zhang, L. Qi, B.-X. Zhao, S. Lian, H.-S. Lv, J. Miao, *Bioorg. Med. Chem. Lett.* **2009**, *19*, 5325–5328.

[33] L.-W. Zheng, Y. Li, D. Ge, B.-X. Zhao, Y.-R. Liu, H.-S. Lv, J. Ding, J.-Y. Miao, *Bioorg. Med. Chem. Lett.* **2009**, *20*, 4766–4770.

[34] Y.-S. Xie, H.-L. Zhao, H. Su, B.-X. Zhao, J.-T. Liu, J.-K. Li, H.-S. Lv, B.-S. Wang, D.-S. Shin, J.-Y. Miao, *Eur. J. Med. Chem.* **2010**, *45*, 210–218.

[35] X.-L. Ding, Y. Xia, L.-J. Wang, X.-F. Zhang, B.-X. Zhao, J.-Y. Miao, *Chin. J. Org. Chem.* **2007**, *27*, 1542–1546.

[36] Z. Tang, X.-L. Ding, W.-L. Dong, B.-X. Zhao, *Acta Cryst. E* **2009**, *65*, o865–o866.

[37] L. Risteli, J. Risteli, *Ann. Med.* **1993**, *25*, 385–393.

[38] A. Yamaguchi, T. Ishizuya, N. Kintou, Y. Wada, T. Katagiri, J. M. Wozney, V. Rosen, S. Yoshiki, *Biochem. Biophys. Res. Commun.* **1996**, *220*, 366–371.

[39] H. Robson, T. Siebler, D. A. Stevens, S. M. Shalet, G. R. Williams, *Endocrinology* **2000**, *141*, 3887–3897.

[40] S.-Y. Jiang, R. Shu, Z.-C. Song, Y.-F. Xie, *Cell Prolif.* **2011**, *44*, 372–379.

[41] C. Mangano, F. Paino, R. d'Aquino, A. De Rosa, G. Iezzi, A. Piattelli, L. Laino, T. Mitsiadis, V. Desiderio, F. Mangano, G. Papaccio, V. Tirino, *PLoS One* **2011**, *6*, e18721.

[42] A. Morozumi, *J. Oral Sci.* **2011**, *53*, 509–516.

[43] G. M. Sheldrick, **1997**, *SHELX-97, Program for the Refinement of Crystal Structures*, University of Goettingen, Goettingen, Germany.

